DHODH inhibitors sensitize cancer cells to ferroptosis via FSP1 inhibition

Eikan Mishima
Helmholtz Zentrum Muenchen https://orcid.org/0000-0002-3706-2745
Toshitaka Nakamura
Helmholtz Zentrum Muenchen https://orcid.org/0000-0002-4248-2058
Jiashuo Zheng
Helmholtz Zentrum Muenchen https://orcid.org/0000-0002-5387-1358
Weijia Zhang
Helmholtz Zentrum Muenchen
André Santos Dias Mourão
Helmholtz Zentrum Muenchen https://orcid.org/0000-0003-0764-9868
Peter Sennhenn
transMedChem https://orcid.org/0000-0001-9639-8532
Marcus Conrad (marcus.conrad@helmholtz-muenchen.de)
Helmholtz Zentrum Muenchen https://orcid.org/0000-0003-1140-5612

Short Report

Keywords: Ferroptosis, DHODH, FSP1, ubiquinone, brequinar

Posted Date: October 24th, 2022

DOI: https://doi.org/10.21203/rs.3.rs-2190326/v1

DHODH inhibitors sensitize cancer cells to ferroptosis via FSP1 inhibition

Eikan Mishima[1,2§], Toshitaka Nakamura[1§], Jiashuo Zheng[1§], Weijia Zhang[1], André Santos Dias Mourão[3], Peter Sennhenn[4], Marcus Conrad[1]

1. Institute of Metabolism and Cell Death, Helmholtz Zentrum München, Neuherberg, Germany
2. Division of Nephrology, Rheumatology and Endocrinology, Tohoku University Graduate School of Medicine, Sendai, Japan
3. Institute of Structural Biology, Helmholtz Zentrum München, Neuherberg, Germany
4. *trans*MedChem, Munich, Germany

§, Equal contribution: EM, TN and JZ.

*Correspondence: marcus.conrad@helmholtz-muenchen.de

The quest for novel targets breaking cancer therapeutic resistance has led to exciting efforts to leverage ferroptosis specifically in cancer cells, traditionally vulnerable to iron-dependent lipid peroxidation[1]. In a recent paper published in this venue, Mao *et al.*[2] introduced mitochondrially localized dihydroorotate dehydrogenase (DHODH) as an enzyme mediating ferroptosis resistance in tumor cells by reducing mitochondrial ubiquinone (CoQ_{10}), which in turn facilitates scavenging of oxygen radicals in mitochondrial membranes.

Canonically, DHODH catalyzes the ubiquinone-dependent oxidation of dihydroorotate to orotate, an essential building block for the *de novo* pyrimidine biosynthesis required during cell proliferation and therefore presents an attractive target for tumor therapy[3] (**Extended Data Fig. 1a**). Mao *et al.* claim that in addition to the "mitochondrial form" of glutathione peroxidase 4 (GPX4), DHODH is able to suppress ferroptosis at the inner mitochondrial membrane by reducing ubiquinone to ubiquinol, and therefore postulate that DHODH constitutes a druggable target for ferroptosis sensititazion[2]. Substantiating their conclusions, the authors showed that cancer cell lines genetically lacking *DHODH* were more sensitive to ferroptosis-inducing agents including the GPX4 inhibitor (*1S,3R*)-RSL3 (RSL3). Moreover, they showed brequinar, a potent and selective inhibitor of DHODH, also sensitized cancer cells toward ferroptosis. While a comprehensive mechanistic framework explaining which molecular events ultimately determine the cells' sensitivity to ferroptosis constitutes a central goal for the ferroptosis field, the study by Mao *et al.* contains several weaknesses and misinterpretations, strongly arguing against the conclusion that inhibition of DHODH is a promising target to overcome ferroptosis resistance in cancer cells.

First, the authors used extremely high concentrations of brequinar (i.e., 500 µM) exceeding by far the reported IC_{50} (i.e., 7 nM) to inhibit DHODH[3,4]. Although we could indeed observe a synergistic effect of brequinar and ferroptosis inducers, including RSL3, in various cancer cells (**Fig. 1a and Extended Data Fig. 1b-d**), the sensitizing effect of brequinar was only evident at a high concentration (IC_{50} = 61 μM, **Fig 1a**), far beyond that required for DHODH inhibition (**Fig. 1b and Extended Data Fig. 1e**). DHODH is a CoQ_{10}-reducing flavoprotein akin to ferroptosis suppressor protein-1 (FSP1), which is another ferroptosis player[5,6]. FSP1 suppresses ferroptosis by reducing extramitochondrial CoQ_{10} (and vitamin K), thereby preventing lipid peroxidation in a wide array of cancer cell lines independently of the cysteine/glutathione/GPX4 axis. Thus, we wondered whether the ferroptosis sensitizing effect of brequinar was actually mediated by inhibition of FSP1 especially in light of the high concentrations used throughout the study by Mao *et al*. Indeed, cell-free assays using recombinant FSP1 revealed that high concentrations of brequinar inhibited FSP1 activity (IC_{50} = 24 and 14 μM for human and mouse FSP1, respectively) like the human FSP1-specific inhibitor iFSP1[5] (**Fig. 1c and Extended Data Fig. 2a-c**). In line with this, the high concentration of brequinar also induced ferroptosis in mouse fibroblasts Pfa1 cells with genetic deletion of *Gpx4* and stably overexpressing human FSP1, whose survival solely depends on FSP1 activity[5] (**Fig. 1d**). Importantly, the ferroptosis sensitizing effect of brequinar was retained regardless of the ablation of DHODH (**Fig. 1e and Extended Data Fig. 2d**), whereas it was lost in *FSP1* knockout cells (**Fig. 1f**). Interestingly, alternative DHODH inhibitors (e.g., vidofludimus) also showed FSP1 inhibitory effects and sensitized cells to ferroptosis (**Extended Data Fig. 2e-h**), while BAY-2402234, a DHODH inhibitor seemingly lacking FSP1 inhibitory activity, failed to sensitize toward ferroptosis (**Extended Data Fig. 2h**). Predictive structure analysis suggested that brequinar fitted well in the putative CoQ_{10}-binding pocket of FSP1 (**Fig. 1g and Extended Data Fig. 2i**). Together, these results demonstrate that the ferroptosis sensitizing effect of brequinar (and several other DHODH inhibitors) is mediated via inhibition of FSP1 but not DHODH.

Second, Mao *et al*. report that genetic deletion of *DHODH* potently sensitized human cancer cells, including HT-1080, to ferroptosis induced by RSL3[2]. Nonetheless, in our hands this sensitizing effect by deletion of DHODH was much less pronounced as they claimed and by far smaller than the effect of *FSP1* deletion (**Fig. 1h and Extended Data Fig. 3a**). This tendency was more apparent in other cancer cell lines (**Fig. 1h**). In addition, unlike FSP1, overexpression of DHODH invariably failed to protect Pfa1 cells from ferroptosis induced by genetic deletion of *Gpx4* or by RSL3 treatment (**Fig. 1i and Extended Data Fig. 3b,c**). By stark contrast, overexpression of FSP1 solely is sufficient to prevent ferroptosis in the absence of GPX4 and DHODH (**Extended Data Fig. 3d,e**). As such, the contribution of DHODH to ferroptosis resistance seems subtle and marginal.

Third, the concentration of RSL3 used by Mao *et al.* to induce ferroptosis in HT-1080 cells was remarkably high. HT-1080 is among the most ferroptosis-sensitive human cancer cell lines and is thus widely used in ferroptosis research. Based on our and other groups' results, 300 nM of RSL3 is generally sufficient to induce ferroptosis in these cells (although fetal bovine serum contained in the culture media may have an impact the ferroptosis sensitivity due to varying concentrations of selenium, vitamin E and/or other micronutrients). Nonetheless, the authors used more than 10 μM of RSL3 to induce ferroptosis in HT-1080 cells[2]. Seemingly these high concentrations were necessary since the authors worked with extraordinarily high cell densities, seeding 20,000 cells per well in a 96-well plate. In light of this peculiarity, it should be highlighted that high cell densities can desensitize cells to ferroptosis and even protect *Gpx4* knockout cells from dying[7,8] (**Extended Data Fig. 3f**). Besides GPX4, RSL3 targets most of the 25 human selenoproteins due to the strong electrophilic nature of the chloroacetamide group of RSL3 towards selenocysteine (which likely becomes even more relevant at higher concentrations as used here; >10 μM)[9], therefore we assumed that the confluent cell culture conditions seem to be suboptimal when examining the ferroptosis sensitivity of the cells against RSL3.

Last, the role of the mitochondrial form of GPX4 in ferroptosis prevention claimed by Mao *et al.* is questionable. Here, it is important to mention that GPX4 is expressed in three distinct isoforms (**Extended Data Fig. 4a**). Transcription of the short form GPX4 (alias cytosolic form) is driven by its own promoter 5′ of exon 1, while the mitochondrial matrix form is driven by a distal promoter, which allows translation of a cognate mitochondrial targeting signal at its N-terminus. Transcription of nuclear GPX4 is mediated by its own promoter in an alternative exon[10]. The short form GPX4 is abundantly expressed in all tissues and is enriched in the cytoplasm and the extra-matrix space of mitochondria of somatic cells, while the mitochondrial matrix and nuclear forms are abundantly expressed in the mitochondrial matrix and nucleus of testicular cells, respectively[11,12] (**Extended Data Fig. 4b**). Earlier studies using isoform-specific knockout and transgenic mice as well as cells showed that both the mitochondrial matrix and nuclear form are important for spermatogenesis, but are otherwise dispensable for cytoprotection[12-14]. Intriguingly, although Mao *et al.* first reported that mitochondrial GPX4 plays a role in ferroptosis prevention[2], a subsequent report by the same authors' group reconciles their findings by showing that ferroptosis induced by *GPX4* deletion can only be prevented by overexpression of the cytosolic GPX4 (i.e., the short form), but not the mitochondrial matrix form[15], which is in agreement with our data (**Extended Data Fig. 4c**). In addition, across a range of cancer cell lines the mitochondrial matrix form of GPX4 was expressed at a much lower level than the short form, as determined by quantitative RT-PCR, the only way to unequivocally discriminate between the two forms (**Extended Data Fig. 4d**), similar to earlier study on mouse tissues[11].

In sum, DHODH inhibitors including brequinar at higher concentrations sensitize cancer cells to ferroptosis via inhibition of FSP1 but not DHODH. Appropriate concentrations of both ferroptosis-inducing and -sensitizing compounds are mandatory to avoid off-target effects. Although a number of DHODH inhibitors have been developed in the past and are in clinical development against solid and hematological malignancies[3], our study infers that both the concentration and the target engagement of DHODH inhibitors need to be carefully evaluated. Furthermore, we reiterate the importance of cell density in ferroptosis study and the irrelevant role of mitochondrial matrix GPX4 in ferroptosis prevention. The contribution of DHODH in ferroptosis, however, seems to be minor and context-dependent at best.

References

1 Jiang, X., Stockwell, B. R. & Conrad, M. Ferroptosis: mechanisms, biology and role in disease. *Nat Rev Mol Cell Biol* **22**, 266-282, doi:10.1038/s41580-020-00324-8 (2021).

2 Mao, C. *et al.* DHODH-mediated ferroptosis defence is a targetable vulnerability in cancer. *Nature* **593**, 586-590, doi:10.1038/s41586-021-03539-7 (2021).

3 Zhang, L. *et al.* Recent advances of human dihydroorotate dehydrogenase inhibitors for cancer therapy: Current development and future perspectives. *Eur J Med Chem* **232**, 114176, doi:10.1016/j.ejmech.2022.114176 (2022).

4 Baumgartner, R. *et al.* Dual binding mode of a novel series of DHODH inhibitors. *J Med Chem* **49**, 1239-1247, doi:10.1021/jm0506975 (2006).

5 Doll, S. *et al.* FSP1 is a glutathione-independent ferroptosis suppressor. *Nature* **575**, 693-698, doi:10.1038/s41586-019-1707-0 (2019).

6 Mishima, E. *et al.* A non-canonical vitamin K cycle is a potent ferroptosis suppressor. *Nature*, doi:10.1038/s41586-022-05022-3 (2022).

7 Seiler, A. *et al.* Glutathione peroxidase 4 senses and translates oxidative stress into 12/15-lipoxygenase dependent- and AIF-mediated cell death. *Cell Metab* **8**, 237-248, doi:10.1016/j.cmet.2008.07.005 (2008).

8 Wu, J. *et al.* Intercellular interaction dictates cancer cell ferroptosis via NF2-YAP signalling. *Nature* **572**, 402-406, doi:10.1038/s41586-019-1426-6 (2019).

9 Chen, Y. *et al.* Quantitative Profiling of Protein Carbonylations in Ferroptosis by an Aniline-Derived Probe. *J Am Chem Soc* **140**, 4712-4720, doi:10.1021/jacs.8b01462 (2018).

10 Moreno, S. G., Laux, G., Brielmeier, M., Bornkamm, G. W. & Conrad, M. Testis-specific expression of the nuclear form of phospholipid hydroperoxide glutathione peroxidase (PHGPx). *Biol Chem* **384**, 635-643, doi:10.1515/BC.2003.070 (2003).

11 Schneider, M. *et al.* Embryonic expression profile of phospholipid hydroperoxide glutathione peroxidase. *Gene Expr Patterns* **6**, 489-494, doi:10.1016/j.modgep.2005.11.002 (2006).

12 Liang, H. *et al.* Short form glutathione peroxidase 4 is the essential isoform required for survival and somatic mitochondrial functions. *J Biol Chem* **284**, 30836-30844, doi:10.1074/jbc.M109.032839 (2009).

13 Conrad, M. *et al.* The nuclear form of phospholipid hydroperoxide glutathione peroxidase is a protein thiol peroxidase contributing to sperm chromatin stability. *Mol Cell Biol* **25**, 7637-7644, doi:10.1128/MCB.25.17.7637-7644.2005 (2005).

14 Schneider, M. *et al.* Mitochondrial glutathione peroxidase 4 disruption causes male infertility. *FASEB J* **23**, 3233-3242, doi:10.1096/fj.09-132795 (2009).

15 Wu, S. *et al.* A ferroptosis defense mechanism mediated by glycerol-3-phosphate dehydrogenase 2 in mitochondria. *Proc Natl Acad Sci U S A* **119**, e2121987119, doi:10.1073/pnas.2121987119 (2022).

Figure legends

Fig. 1 | Brequinar sensitizes cancer cells to ferroptosis via FSP1 inhibition.

a. (Left) Heatmap of viability of HT-1080 cells showing the synergistic lethal effects of brequinar (BQR) and RSL3. The well-established ferroptosis inhibitor liproxstatin-1 (Lip1, 0.5 μM) was used as a positive control to prevent ferroptosis. (Middle) Viability of HT-1080 cells treated with varying concentrations of RSL3 and a fixed concentration of BQR (100 μM) for 24 h. (Right) Viability of HT-1080 cells treated with increasing concentrations of BQR and a sub-lethal dose of RSL3 (0.01 μM) for 24 h.

b. (Left) Relative cell counts of BQR-treated HT1080 cells incubated with or without uridine (100 μM) for 5 days. (Right) In vitro assays showing the inhibitory effect of BQR (0.1 and 1 μM) on DHODH enzyme activity. Recombinant human DHODH (hDHODH, 25 nM), dihydroorotate (DHO), coenzyme Q_0 (COQ_0), 2,6-dichloroindophenol (DCIP) were used.

c. In vitro assays showing the inhibitory effect of BQR and iFSP1 toward FSP1 enzyme activity. Recombinant human FSP1 (hFSP1, 50 nM) was used.

d. The effect of BQR on the viability of mouse embryonic fibroblasts Pfa1 cells with genetic deletion of *Gpx4* and stably overexpressing human FSP1.

e. The synergistic effect of BQR (100 μM) and RSL3 on the viability of *DHODH* knockout (KO) HT-1080 cells with or without overexpression (OE) of human DHODH.

f. The effect of BQR (200 μM) and iFSP1 (5 μM) on the viability of 786-O cells wildtype (WT) or KO for either *DHODH* or *FSP1*.

g. Chemical structures of BQR and iFSP1 and the binding prediction of BQR in the hFSP1 enzyme.

h. The effects of the genetic KO of *DHODH* or *FSP1* on the viability of HT-1080, 786-O, A375 and MDA-MB-436 cancer cell lines treated with RSL3 for 24 h.

i. Viability of wild type or 4-hydroxytamoxifen (TAM)-induced *Gpx4* KO Pfa1 cells stably overexpressing HA-tagged hFSP1 or hDHODH. (Left) Viability was measured three days after TAM treatment. (Right) Viability was measured after treatment with RSL3 for 24 h.

Data are mean ± s.d. of n = 3 (a, b (left), d-f, h and i). Data is representative of two (b, right) and three independent experiments (c), respectively.

Extended Data Fig. 1 | The synergistic effect of brequinar with ferroptosis inducers in a panel of cancer cell lines.

a. Known DHODH inhibitors in cancer-related clinical trials. Sourced from https://clinicaltrials.gov/, August 2022.

b. Heatmaps of cell viability showing the synergistic effects of brequinar (BQR) with ML210, erastin and BSO in HT-1080 cells. Viability was measured after 48 h (ML210 and erastin) and 72 h treatment (BSO).

c. Heatmaps of cell viability showing the synergistic effects of BQR with RSL3 and ML210 in 786-O, A375, MDA-MB-436 and A549 cells. Viability was measured after 48 h.

d. Evaluation of cellular toxicity of brequinar. HT-1080, 786-O and MDA-MB-436 cells were treated with indicated concentrations of BQR with or without the ferroptosis inhibitor liproxstatin-1 (Lip1, 1 μM) for 24 h. BQR treatment alone was not sufficient to induce ferroptosis.

e. Representative images of HT-1080 cells treated with or without BQR (1 μM) and uridine (100 μM) for 5 days. The cells were seeded at a density of 200 cells/well in 96 well plate.

Data is mean ± s.d. of n = 3 (d). Data is representative of two independent experiments (b-e)

Extended Data Fig. 2 | Inhibitory effects of DHODH inhibitors against FSP1 enzyme activity.

a. (Left) Scheme of the FSP1 enzyme activity assay. Resazurin (100 μM), a substrate of FSP1, is reduced to resorufin by incubation with recombinant FSP1 protein (50 and 40 nM of human and mouse FSP1, respectively) and NADH (200 μM). The amount of resorufin evaluated by fluorescent intensity (ex 540/em 590 nm) indicates FSP1 enzymatic activity. (Right) Scheme of the DHODH enzyme activity assay. Enzyme reaction of recombinant human DHODH (25 nM), dihydroorotate (DHO, 500 μM) and CoQ_0 (100 μM) reduces an electron acceptor 2, 6-dichlorophenolindophenol (DCIP, 120 μM) to $DCIPH_2$. Absorbance change of DCIP (at absorbance 610 nm) indicates DHODH enzymatic activity.

b. NADH consumption assay using recombinant human FSP1 protein (25 nM) in combination with or without brequinar (BQR, 300 μM). Menadione (50 μM) was used as a substrate of FSP1. Brequinar inhibited the FSP1-dependent NADH consumption.

c. The inhibitory effect of BQR and iFSP1 on mouse FSP1 enzymatic activity.

d. Heatmaps showing the viability and immunoblotting of hFSP1-overexpressed (OE) and *Dhodh* KO-Pfa1 cells with or without overexpression of hDHODH. Combination of RSL3 with BQR synergistically induced cell death in both cell lines.

e. The inhibitory effect of known DHODH inhibitors on human and mouse FSP1 enzyme activity.

f. Calculated IC_{50} values of iFSP1 and DHODH inhibitors against human and mouse FSP1.

g. The inhibitory effect of DHODH inhibitors against human DHODH enzymatic activity.

h. Heatmaps showing the viability of HT-1080 cells (5,000 cells per well) treated with RSL3 in combination with vidofludimus or BAY-2402234 for 24 h. The values of the groups treated with zero or 0.01 μM of RSL3 are also shown as the right graphs.

i. The binding prediction of iFSP1 in human FSP1 protein. Data is mean ± s.d. of n = 3 (b). Data is representative of three (b, c and e) and two independent experiments (d, g and h), respectively.

Extended Data Fig. 3 | Immunoblotting of genetic deletion or overexpression of FSP1 and DHODH, and the effect of cell density on ferroptosis sensitivity.

a. Immunoblotting of lysates of *FSP1* KO and *DHODH* KO cells using HT-1080, 786-O, A375 and MDA-MB-436 cell lines. Each parental cells were used as wild type (WT).

b. Immunoblotting of lysates of Pfa1 cells with stable overexpression (OE) of C-terminally HA-tagged human DHODH (hDHODH) or FSP1 (hFSP1).

c. Relative cell counts of *Dhodh* KO Pfa1 cells with or without stable OE of hDHODH seeded 200 cells/well in 96 well plate and incubated with or without uridine (50 μM) for 5 days. hDHODH OE rescued the suppression of cell growth in *Dhodh* KO Pfa1 cells without uridine supplementation.

d. Immunoblotting of lysate and viability of A375 cells of WT, *GPX4* KO, *GPX4* KO with hFSP1 OE and *GPX4/DHODH* double KO with hFSP1 OE. For the measurement of cell viability, 500 cells/well were seeded in 96 well plate and incubated with or without Lip1 (1 μM) for 4 days. Viability of the cells incubated with Lip1 (1 μM) was taken as 100%.

e. Immunoblotting of lysate and viability of *Gpx4* and *Dhodh* double KO Pfa1 cells with stable OE of hFSP1. The cells were seeded at a density of 300 cells/well in 96 well plate and incubated with or without uridine (50 μM) and Lip1 (1 μM) for 5 days. The *Gpx4* and *Dhodh* double KO Pfa1 cells with OE of hFSP1 cells can survive without Lip1.

f. The effect of cell density of HT-1080 cells on RSL3-induced cell death. The cells were seeded at densities of 3,000, 8,000 or 20,000 cells/well in a 96 well plate. On the next day, the cells were treated with RSL3 for 6 h and viability was determined. Data is mean ± s.d. of n = 9 (c) and n = 3 (d-f). Two-tailed *t*-test (c); one-way ANOVA with Dunnett's test (d).

Extended Data Fig. 4 | Expression pattern and subcellular localization of GPX4 isoforms.

a. Structural organization of the *GPX4* gene, mRNA and protein of the GPX4 isoforms. Arrows indicate the transcription initiation sites. The dashed lines indicate the different splicing variants. ATG indicates the initiation methionine codon. MTS, mitochondrial targeting sequence; NLS, nuclear localization signal. The N-terminus of nuclear GPX4 contains an NLS and protamine-like DNA binding motives allowing the enzyme to bind to sperm DNA, enabling its thiol peroxidase function.

b. A scheme depicting the reported subcellular localization of each GPX4 isoform in somatic and testicular cells. The short form is abundantly expressed in the cytoplasm and mitochondrial extra-matrix space of somatic cells, while the mitochondrial matrix form is abundantly expressed in the mitochondrial matrix of testicular cells.

c. Viability of *GPX4* KO HT-1080 cells (500 cells/well) overexpressing the short or mitochondrial matrix form of GPX4 for three days after withdrawal of ferrostatin-1 (a ferroptosis inhibitor). The cells were prepared by infection with the indicated serial dilution of lentiviral particles containing the expression plasmids. Immunoblotting validated the overexpression of each form. Viability of the cells incubated with Lip1 (1 μM) was taken as 100%.

d. The design of the primer pairs detecting both the short and mitochondrial matrix forms (106 bp) and specific for the mitochondrial matrix form (196 bp). Agarose gel images showing the amplification of the specific single band. The ratio of the mitochondrial matrix form/short and mitochondrial matrix forms of *GPX4* mRNA expression in the cancer cell lines was calculated as $2^{-\Delta CT}$ in quantitative RT-PCR. Data is representative of two independent experiments (c and d). Data is mean ± s.d. of n = 3 (c and d).

Materials and Methods

Chemicals

Brequinar (SML0113), uridine (U3750), resazurin sodium salt (R7017), NADH (N8129), coenzyme Q_0 (D9150), 2,6-dichloroindophenol (DCIP, D1878), L-dihydroorotic acid (D7128), L-buthionine sulfoximine (BSO; B2515), menadione (M5625), and ferrostatin-1 (Fer1, SML0583) were purchased from Sigma-Aldrich. *(1S,3R)*-RSL3 (19288), ML210 (23282), vidofludimus (18377), BAY-2402234 (33259), and ASLAN003 (33516) were purchased from Cayman. The following chemicals were obtained as indicated: erastin (329600, Merck Millipore), iFSP1 (8009-2626, ChemDiv), liproxstatin-1 (Lip1, S7699, Selleckchem), PCT299 (HY-124593, MedChemExpress).

Cell lines

4-hydroxy-tamoxifen (TAM)-inducible *Gpx4*$^{-/-}$ murine immortalized fibroblasts (Pfa1) were reported previously[8]. HT-1080 (CCL-121), 786-O (CRL-1932), A375 (CRL-1619), MDA-MB-436 (HTB-130), A549 (CCL-185), H460 (HTB-177), SW620 (CCL-227) and HEK293T (CRL-3216) cells were obtained from ATCC. LOX-IMVI was obtained from NCI/NIH. Cell lines, except for MDA-MB-436 and H460, were maintained in DMEM high glucose (4.5 g glucose/L, 21969-035, Gibco) supplemented with 10% fetal bovine serum (FBS), 2 mM *L*-glutamine, and 1% penicillin/streptomycin at 37 °C with 5% CO_2. MDA-MB-436 and H460 cells were maintained in RPMI 1640 medium (61870-010, GlutaMAX supplemented, Gibco) supplemented with 10% FBS and 1% penicillin/streptomycin. *DHODH* knockout (KO) cells and *Dhodh* KO Pfa1 cells were maintained in a medium containing uridine (100 and 50 µM, respectively). *GPX4* KO cells were maintained in a medium containing Lip1 (1 µM). All cells were regularly tested for mycoplasma contamination.

Cell viability assays

Cells were seeded on 96-well plates at the following cell number per well and allowed to adhere overnight. For RSL3 treatment, 3,000 cells (HT-1080, 786-O and A375), 5,000 cells (MDA-MB-436) and 1,500 cells (Pfa1) were seeded. For the viability assay shown in a heatmap, cells were seeded at 2,500 cells (HT-1080, 786-O, A375 and A549) and 5,000 cells (MDA-MB-436) for RSL3, ML210 and erastin treatment; and 1,000 cells of HT-1080 per well for BSO treatment. On the next day, cells were treated with the ferroptosis inducers. In the cotreatment experiments, brequinar, iFSP1 or Lip1 were added alongside with the ferroptosis inducers. When brequinar was used in the assay, uridine (100 μM) was supplemented in the media to avoid the effect of the depletion of intracellular pyrimidines as well as to maintain *DHODH* KO cells. Cell viability was assessed 24 h (RSL3 and ML210), 48 h (erastin) and 72 h (BSO) after the treatment using AquaBluer (MultiTarget Pharmaceuticals) or 0.004 % Resazurin sodium salt (Sigma Aldrich) unless stated otherwise. The cell viability was expressed as relative values compared to the control sample, which was defined as 100%. To induce the KO of *Gpx4* in Pfa1 cells, the cells were seeded on 96-well plates (500 cells/well) and treated with 1 μM TAM. Cell viability of TAM-treated Pfa1 cells was assessed 72 h after the treatment. To evaluate the effect of the confluency of cells towards ferroptosis sensitivity, HT-1080 cells were seeded on 96-well plates at 3,000, 8,000 and 20,000 cells per well, and then treated with RSL3 on the following day.

Cell proliferation assays

HT-1080 and Pfa1 cells were seeded on 96-well plates at 200 cells/well and incubated with or without uridine (100 and 50 μM, respectively) for 5 days. After the incubation, relative cell counts were evaluated using AquaBluer.

Preparation of lentiviral particles

Lentiviral packaging system consisting of a transfer plasmid, psPAX2 (12260, Addgene), with pMD2.G (for human cells, 12259, Addgene) or pHCMV-EcoEnv (for mouse cells, 15802, Addgene) was co-lipofected into HEK293T cells using PEI-MAX (Polysciences). Cell culture supernatants containing viral particles were harvested 48 h after the transfection and used to transduce the cell line of interest after filtration using a 0.45 μm low protein binding syringe filter.

CRISPR/Cas9-mediated gene knockout

Sequences of single guide RNAs (sgRNA), vectors for expression of Cas9 and sgRNA, and Cas9 expression system are listed in Supplementary Table 1. For transient expression of the CRISPR/Cas9 system, cells were transiently co-transfected with the sgRNA-cloned Cas9 expression plasmids (listed in Supplementary Table 1) using the X-tremeGENE HP agent (Roche). One day after transfection, cells were selected by treatment with puromycin (1 μg/mL), blasticidin (10 μg/mL) and/or geneticin (1 mg/mL). After selection, single-cell clones were picked and knockout clones were identified by immunoblotting. For stable expression of the CRISPR/Cas9 System, cells were infected with lentiviral particles containing the sgRNA-cloned lentiCRISPRv2-neo plasmid (98292, Addgene) with protamine sulfate (8 μg/mL). One day after transfection, cells were treated with geneticin (1 mg/mL). After the selection, loss of expression of the targeted protein was confirmed by immunoblotting of batch cultures. For Doxycycline (Dox)-inducible Cas9 expression system, Dox-inducible Cas9 expressing cells were generated by transducing lentiviral particles containing pCW-Cas9-Blast (83481, Addgene)[6]. pCW-Cas9-Blast expressing cells were infected with lentiviral particles containing the sgRNA-cloned LentiGuide-Neo (139449, Addgene) or pKLVU6gRNA(*Bbs*I)-PGKpuro2aBFP vector (50946, Addgene). One day after transfection, cells were treated with geneticin (1 mg/mL) or puromycin (1 μg/mL), and then incubated with Dox (10 μg/mL) for 5 days to express Cas9. After the selection and the

Cas9 induction, single-cell clones were picked and knockout clones were identified by immunoblotting.

Overexpression of DHODH, FSP1 and GPX4 isoforms

Codon-optimized human *DHODH* gene with a C-terminal HA tag was synthesized (Twist Bioscience) and cloned in the expression vector pLV-EF1a-IRES-Neo (85139, Addgene). Human *FSP1*-coding original sequence (NM_001198696.2) with a C-terminal HA tag was cloned in the expression vector p442-Blast. Coding sequences of the short form (NM_001367832.1) and mitochondrial matrix form (NM_002085.5) of human *GPX4* were amplified by PCR using cDNA produced from A375 cells, and they were cloned into the expression vector p442-Blast. Cells were infected with lentiviral particles containing the transfer plasmids. One day after infection, cells were selected with geneticin (1 mg/mL) or blasticidin (10 μg/mL). Reconstitution of DHODH, FSP1 and GPX4 isoforms expression was verified by immunoblotting. *GPX4* KO HT-1080 cells overexpressing each form of GXP4 was maintained with Fer-1 (5 μM) after the selection.

Western blotting

Cells were lysed in LCW lysis buffer pH 7.5 (0.5% Triton X-100, 0.5% sodium deoxycholate salt, 150 mM NaCl, 20 mM Tris-HCl, 10 mM EDTA, 30 mM Na-pyrophosphate tetrabasic decahydrate) containing protease and phosphatase inhibitor mixture (cOmplete and phoSTOP, Roche), and centrifuged at 15,000×g, 4 °C for 20 min. The supernatant was collected and used as the protein sample. Western blotting was performed by standard immunoblotting procedure with 12% SDS-PAGE gel, PVDF membrane, and primary antibodies against human FSP1 (1:1000, sc-377120, Santa Cruz), DHODH (1:1000, sc-166348, Santa Cruz), HA (1:1000, clone 3F10, rat IgG1, developed in-house), and valosin containing protein (VCP for a loading control, 1:10000, ab109240, Abcam). Images were analyzed with Image Lab 6.0 software (Bio-Rad).

Expression and purification of recombinant FSP1 and DHODH

Recombinant human and mouse FSP1 protein containing a N-terminal 6-histidine tag were produced in *Escherichia coli* (*E.coli*) and purified by affinity chromatography with a Ni-NTA system as described previously[5]. Codon optimized DNA sequence corresponding to the mitochondrial intermembrane region of human DHODH 29-395 was synthesized as a gBlocks gene fragment (Integrated DNA Technologies) and cloned into a petM11 vector that contains a N-terminal 6-histidine tag. Expression and purification were done as previously reported[16]. In short, *E.coli* BL21 cells were transformed with the prepared DHODH vector and grown in TB at 37°C. When the cells reached OD 2.0, 0.5 mM IPTG was added and expression was performed at 20°C overnight. Cells were harvested, dissolved in the lysis buffer (PBS supplemented with 10 mM imidazol) and lysed using a sonicator. After centrifugation, the supernatant fraction was applied to a prepacked nickel column and washed extensively with the lysis buffer. The protein was eluted with PBS supplemented with 350 mM imidazole followed by concentration and a final purification step over a size exclusion chromatography column pre-equilibrated with PBS. Protein was aliquoted, frozen in liquid nitrogen and stored at -80°C until further usage.

FSP1 enzyme inhibitor assay

Enzyme reactions in PBS pH 7.4 containing 50 nM hFSP1 or mFSP1 enzyme, 200 µM NADH (freshly prepared in water) and the inhibitors were prepared[6]. After the addition of 100 µM resazurin sodium salt, fluorescent intensity (ex 540/em 590 nm) was measured every 30 sec on a 96-well plate using a SpectraMax M5 Microplate Reader (Molecular devices).

Determination of FSP1 activity by measuring NADH consumption

Enzyme reactions in PBS pH 7.4 containing 25 nM hFSP1 and 50 µM of menadione with or without 300 µM of brequinar were prepared[6]. After the addition of 200 µM NADH, the absorbance at 340 nm was measured every 30 sec on a 96-well plate. Reactions without NADH/without enzyme were used to normalize the results.

DHODH enzyme inhibitor assay

DHODH activity was measured as reported previously[17]. The reaction was performed at pH 8.0 at 32°C in a buffer containing 50 mM Tris, 0.1% Triton X-100, 150 mM NaCl, 25 nM recombinant human DHODH protein, 500 μM L-dihydroorotic acid, 100 μM coenzyme Q_0 and 120 μM DCIP with the inhibitors. DHODH activity was measured kinetically as a function of decreased DCIP absorbance at 600 nm.

***In silico* modeling**

Predictive human FSP1 structure was obtained from AlphaFold2 database (https://alphafold.ebi.ac.uk)[18]. To yield the superposed structure of FSP1 with its cofactor flavin adenine dinucleotide (FAD), the structure of yeast ortholog structure, NDH-2 (Ndi1)[19] (PDB: 4G73) was aligned to FSP1 using Pymol v2.5.2 (Schrödinger), and the position of FAD was extracted and embedded into FSP1 structure as a template for modeling. The modeling software SeeSAR seeSAR v12.1 (BioSoveIT) was employed to dock the selected molecules into the hFSP1 protein. The binding site was detected and defined employing the integrated DoGSiteScorer module embedded in SeeSAR. Molecules were uploaded as SD files without any further preparation. For docking, the number of poses for each molecule was set to 500, and clash tolerance set to high to allow a comparably tolerant generation of poses. The subsequent HYDE scoring function within SeeSAR was used to post-optimize the docking poses and to assess the estimated affinity. After visual inspection, the most viable poses were selected and filtered for favorable torsion quality and docking poses with unfavorable intra- and intermolecular clashes were removed.

Quantitative RT-PCR

Total RNA was extracted from the cells using RNeasy Mini kit (Qiagen) with genomic DNA removal by RNase-Free DNase set (Qiagen), and was reverse-transcribed using the QuantiTect Reverse Transcription Kit (Qiagen). Human testis mRNA was purchased from Takara-bio (636533) and was reverse-transcribed. Quantitative RT-PCR was performed using PowerUp SYBR Green Master Mix (Thermo Fisher Scientific) with qTOWER^3 G (Analytikjena). All samples were run with triplicates under the following condition:1, 50 ˚C for 2 min; 2, 95 ˚C for 2 min; 3, 95 ˚C for 15 sec; 4, 59.5 ˚C for 15 sec; 5, 72˚C for 1 min; 6, 95˚C 1 sec and cycle from 3 to 5 was repeated for 40 times. Sequences of the primers were following: 5′-TGCTCTGTGGGGCTCTG and 5′-ATGTCCTTGGCGGAAAACTC for detecting the short and mitochondrial matrix forms of *GPX4*; and 5′-ATTGGTCGGCTGGACGAG and 5′-ATGTCCTTGGCGGAAAACTC for specific detection of the mitochondrial matrix form. The expression ratio of (the mitochondrial matrix form)/(the short and mitochondrial matrix forms) of *GPX4* was calculated using the ΔCt method.

Quantification and statistical analysis

Statistical information for individual experiments can be found in the corresponding figure legends. Values are presented as mean ± s.d. Statistical comparisons between groups were analyzed by a two-tailed Student's t-test or one-way ANOVA with Dunnett's post hoc test. Statistical analyses were conducted using GraphPad Prism 9 (GraphPad Software).

Data Availability

All data are available within the article and the supplementary information, and from the corresponding author on reasonable request. Gel source images are shown in Supplementary Fig.

Acknowledgments

We would like to thank Adam Wahida for his critical reading of the manuscript. This work was supported by funding from the Deutsche Forschungsgemeinschaft (DFG) (CO 291/7-1) and the DFG Priority Program SPP 2306 [CO 291/9-1, CO 291/10-1]), the German Federal Ministry of Education and Research (BMBF) FERROPath (01EJ2205B), and the European Research Council (ERC) under the European Union's Horizon 2020 research and innovation programme (grant agreement No. GA 884754) to M.C.; JSPS KAKENHI (20KK0363) to E.M. Alexander von Humboldt Post-Doctoral Fellowship to J.Z; and China Scholarship Council to W.Z.

Author Contribution

E.M., T.N, J.Z., and M.C. conceived the study and wrote the manuscript. E.M., T.N., J.Z., and W.Z. performed the experiments and analysis. A.S.D.M. expressed and purified recombinant FSP1 and DHODH. P.S. performed *in silico* modeling. All authors read and agreed on the content of the paper.

Competing interests

M.C. and P.S. hold patents for some of the compounds described herein, and are co-founders and shareholders of ROSCUE Therapeutics GmbH.

Additional information

Correspondence and requests for materials should be addressed to M.C.

References (continued)

16 Walse, B. *et al.* The structures of human dihydroorotate dehydrogenase with and without inhibitor reveal conformational flexibility in the inhibitor and substrate binding sites. *Biochemistry* **47**, 8929-8936, doi:10.1021/bi8003318 (2008).

17 Christian, S. *et al.* The novel dihydroorotate dehydrogenase (DHODH) inhibitor BAY 2402234 triggers differentiation and is effective in the treatment of myeloid malignancies. *Leukemia* **33**, 2403-2415, doi:10.1038/s41375-019-0461-5 (2019).

18 Varadi, M. *et al.* AlphaFold Protein Structure Database: massively expanding the structural coverage of protein-sequence space with high-accuracy models. *Nucleic Acids Res* **50**, D439-D444, doi:10.1093/nar/gkab1061 (2022).

19 Feng, Y. *et al.* Structural insight into the type-II mitochondrial NADH dehydrogenases. *Nature* **491**, 478-482, doi:10.1038/nature11541 (2012).

Fig. 1

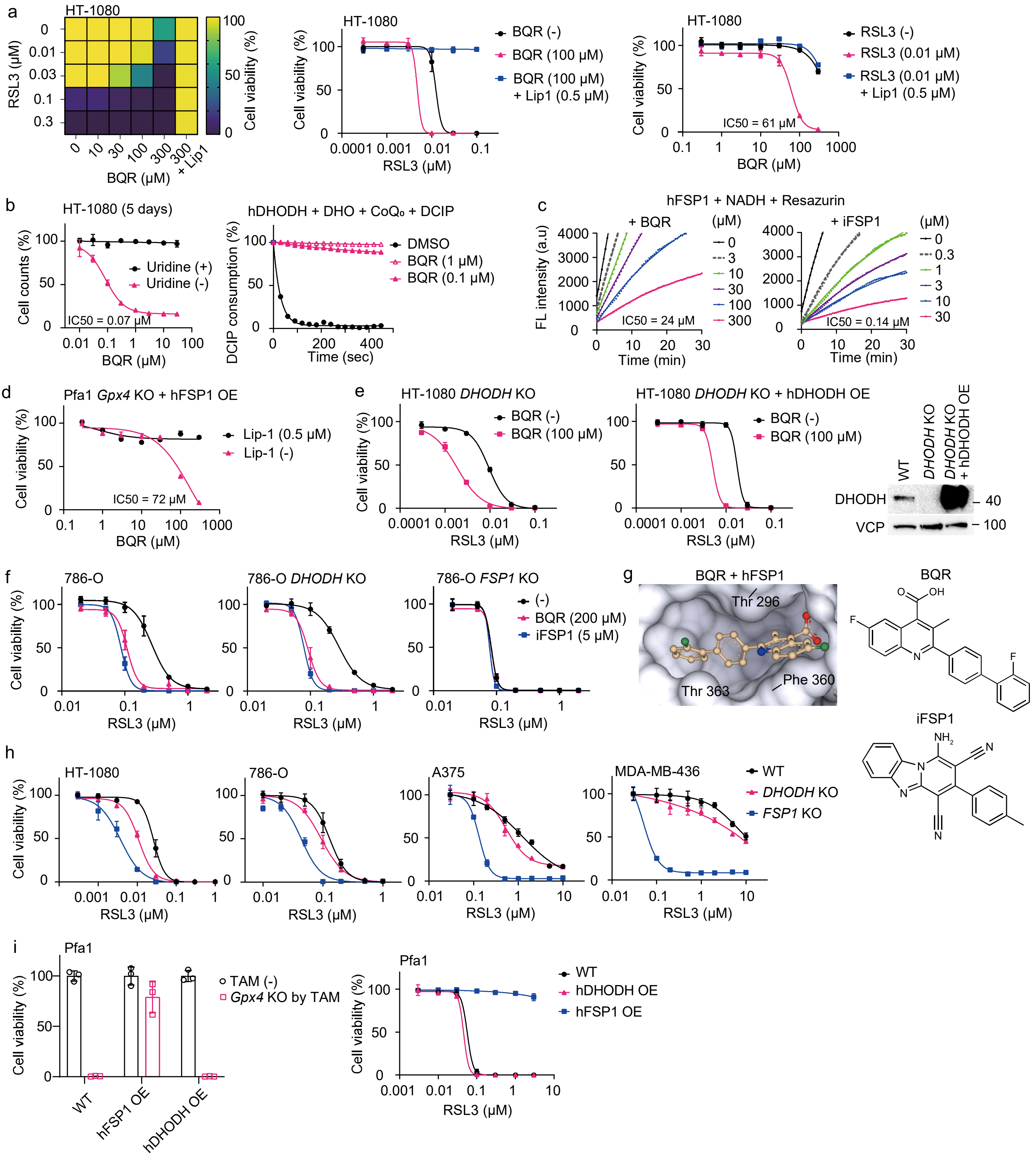
a
HT-1080
RSL3 (μM)
BQR (μM)
Cell viability (%)
HT-1080
BQR (-)
BQR (100 μM)
BQR (100 μM) + Lip1 (0.5 μM)
RSL3 (μM)
HT-1080
RSL3 (-)
RSL3 (0.01 μM)
RSL3 (0.01 μM) + Lip1 (0.5 μM)
IC50 = 61 μM
BQR (μM)
b
HT-1080 (5 days)
Cell counts (%)
Uridine (+)
Uridine (-)
IC50 = 0.07 μM
BQR (μM)
hDHODH + DHO + CoQ₀ + DCIP
DCIP consumption (%)
DMSO
BQR (1 μM)
BQR (0.1 μM)
Time (sec)
c
hFSP1 + NADH + Resazurin
FL intensity (a.u)
+ BQR
(μM)
IC50 = 24 μM
+ iFSP1
(μM)
IC50 = 0.14 μM
Time (min)
d
Pfa1 Gpx4 KO + hFSP1 OE
Lip-1 (0.5 μM)
Lip-1 (-)
IC50 = 72 μM
BQR (μM)
e
HT-1080 DHODH KO
BQR (-)
BQR (100 μM)
HT-1080 DHODH KO + hDHODH OE
BQR (-)
BQR (100 μM)
RSL3 (μM)
WT
DHODH KO
DHODH KO + hDHODH OE
DHODH
VCP
40
100
f
786-O
786-O DHODH KO
786-O FSP1 KO
(-)
BQR (200 μM)
iFSP1 (5 μM)
RSL3 (μM)
g
BQR + hFSP1
Thr 296
Phe 360
Thr 363
BQR
iFSP1
h
HT-1080
786-O
A375
MDA-MB-436
WT
DHODH KO
FSP1 KO
RSL3 (μM)
i
Pfa1
TAM (-)
Gpx4 KO by TAM
WT
hFSP1 OE
hDHODH OE
Pfa1
WT
hDHODH OE
hFSP1 OE
RSL3 (μM)

Extended fig. 1

a

Drug	Disease	Clinical trial	NCT number
Brequinar	Acute myeloid leukemia	Phase I/II	NCT03760666
Vidofludimus			
ASLAN003	Acute myeloid leukemia	Phase II	NCT03451084
PTC299	Acute leukemia	Phase I	NCT03761069
BAY-2402234	Leukemia	Phase I	NCT03404726

b

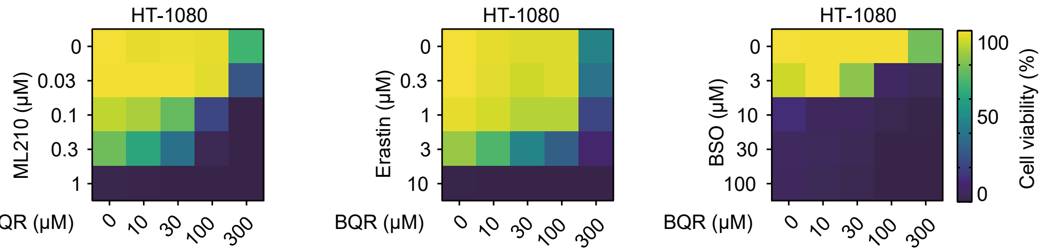

c

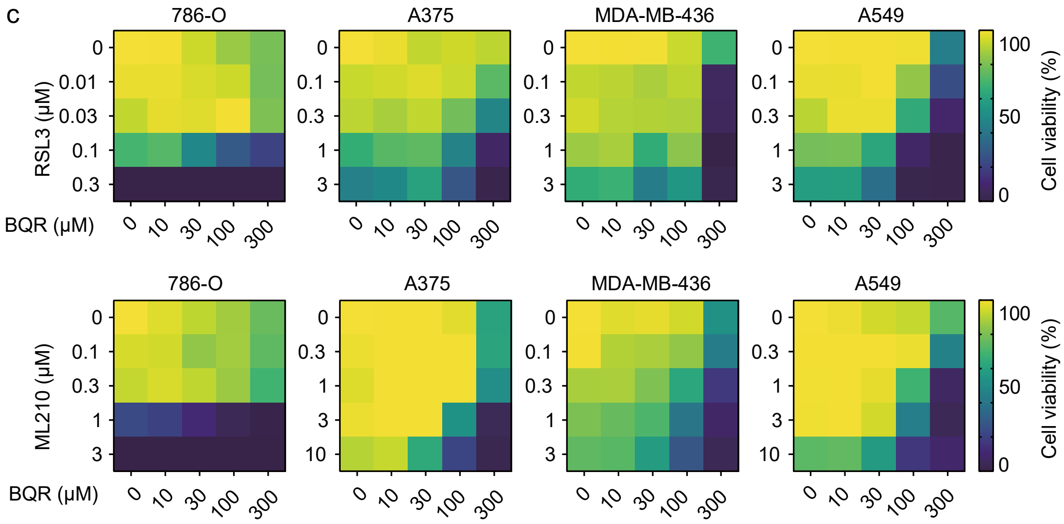

d

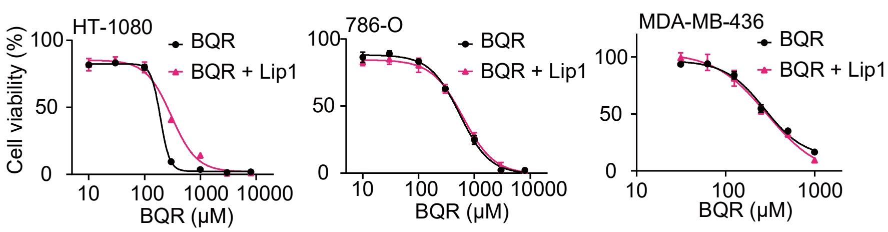

e

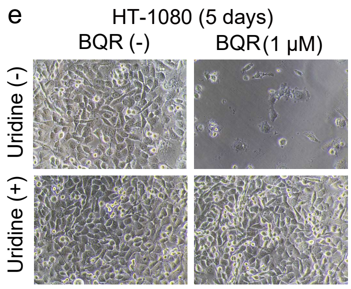

Extended fig. 2

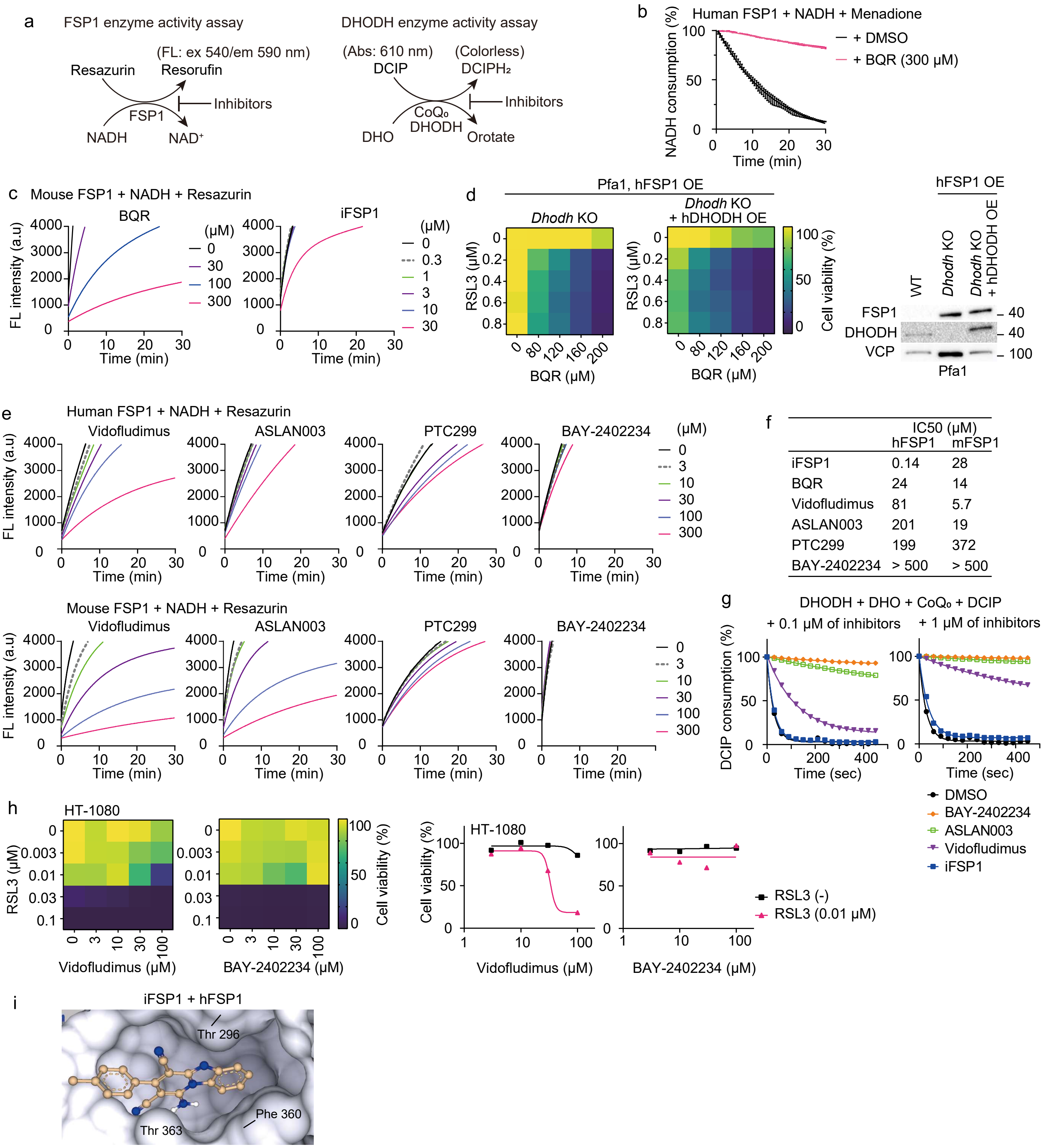

	IC50 (μM) hFSP1	IC50 (μM) mFSP1
iFSP1	0.14	28
BQR	24	14
Vidofludimus	81	5.7
ASLAN003	201	19
PTC299	199	372
BAY-2402234	> 500	> 500

Extended fig. 3

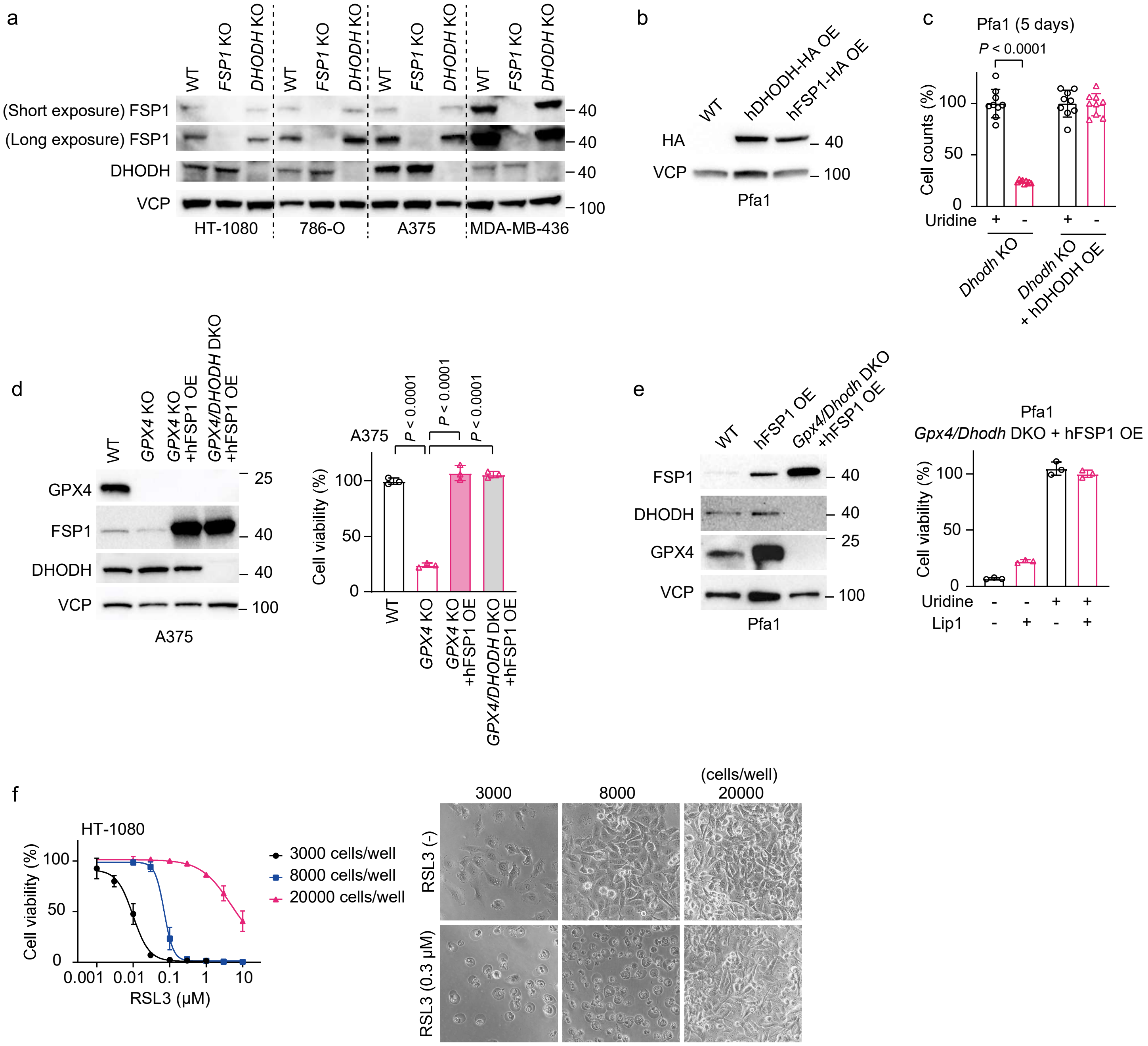

Extended fig. 4